ISBN: 978-3-95450-227-1 ISSN: 2673-5490 doi:10.18429/JACoW-IPAC2022-THPOPT002

BEAM POWER DEPOSITION ON THE CRYOGENIC PERMANENT MAGNET UNDULATOR

L.R. Carver, C. Benabderrahmane, P. Brumund, N. Carmignani, J. Chavanne, G. Le Bec, R. Versteegen, S. White, ESRF, Grenoble, France

Abstract

The ESRF-EBS is currently delivering x-rays with a much higher brilliance and spatial coherence than its predecessor. Within the EBS, there are 5 cryogenic permanent magnet undulators (CPMUs). The magnet blocks for these undulators are operated at 80 K but in general they must be kept at room temperature (300 K) or less or they risk demagnetisation if heated excessively. In the event of a failure of the cryogenic pumps, the ambient magnet temperature increases and they can be further heated by the power induced within the device by the circulating beam. A simulation study was performed to determine the power deposition and temperature rise within the CPMU in order the help define an operational procedure in the event of a cooling failure.

INTRODUCTION

The ESRF-EBS has been commissioned and is currently in operation, delivering high brilliance and high spatial coherence x-rays to the users [1–3]. Within the EBS, there are currently 5 cryogenic permanent magnet undulators (CPMUs) installed and under operation. CPMUs are in-vacuum undulators (IVUs) that are cryogenically cooled to operating temperatures of 80 K. This cooling allows them to achieve higher peak undulator fields (resulting in an improved brilliance for photon energies above 50 keV), while being more resistant to radiation induced demagnetisation, a key feature needed when reducing the minimum gap during operation.

Heating of the magnet blocks can lead to permanent demagnetisation. If there is a failure of the cryogenic cooling during machine operation, the magnets will warm even further due to beam induced heating and could reach temperatures that exceed the safe limit for demagnetisation [4]. Computing the expected temperature rise is therefore an important parameter to be able to safely operate the CPMU.

The CPMU magnet blocks total 2 m in length, with a taper design upstream and downstream to match smoothly the apertures of the surrounding vacuum chamber to the CPMU which has a variable gap setting [6–8]. A photograph of the inside of a CPMU is shown in Fig. 1. The taper has been completely redesigned for the beginning of the EBS, as the previous design showed significant beam induced heating for low gap settings. This prior experience is a strong motivator for this study, as it is needed to confirm if the new taper design is sufficient. The new taper design is shown in Fig. 2.

The power deposited by the beam in the CPMU is a needed input for thermal simulations. To compute the power deposited in the CPMU by the beam a set of impedance simulations was performed in CST Particle Studio [9] and

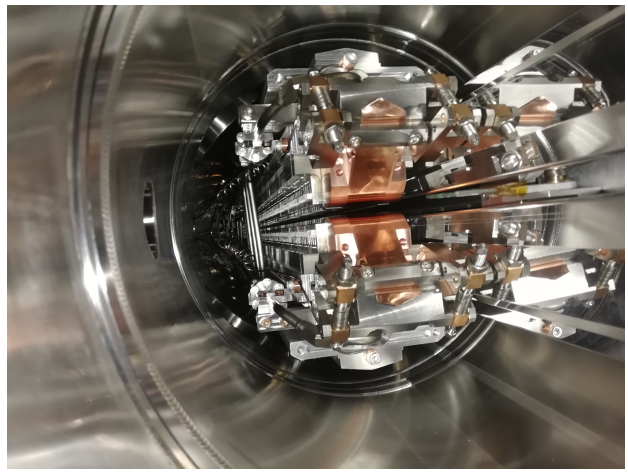

Figure 1: A view inside a CPMU during a bench measurement. A taper is connected at each end to smoothly match the vertical apertures.

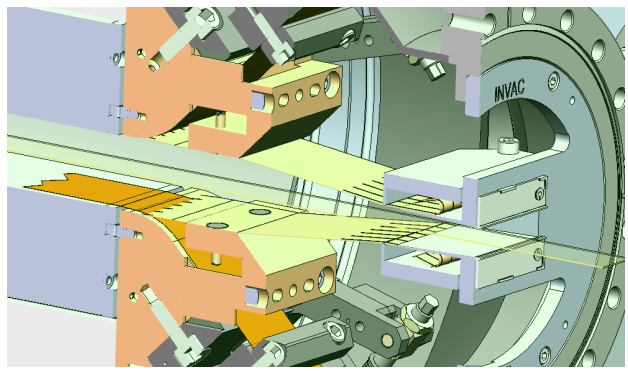

Figure 2: A view of the taper design, the RF fingers can also be seen [5].

Impedance Wake 2D (IW2D) [10]. The details of these impedance simulations will be given in the next section.

COMPUTING THE POWER DEPOSITION

The voltage deposition by a bunched beam in an impedance can be computed from the loss parameter [11,12]

$$\kappa_{\parallel}(\sigma) = \frac{1}{\pi}\int_0^{\infty} d\omega \mathrm{Re}[Z_{\parallel}(\omega)]h(\omega,\sigma), \quad (1)$$

where $Z_{\parallel}$ is the longitudinal impedance and h is the bunch power spectrum, computed from

$$\lambda(\omega) = \exp[-\frac{\omega^2\sigma_{\omega}^2}{2}], \quad (2)$$

where σ is the bunch length and therefore

$$h(\omega) = \lambda(\omega)\lambda^*(\omega). \quad (3)$$

ISBN: 978-3-95450-227-1 ISSN: 2673-5490 doi:10.18429/JACoW-IPAC2022-THPOPT002

The power deposition can be computed from

$$P = \frac{N\kappa_{\parallel} I_b^2}{f_0}, \quad (4)$$

where f_0 is the revolution frequency, N is the number of bunches and I_b is the bunch current.

These formula simply compute the power deposition coming from a single bunch and then this is multiplied by the number of bunches. As a verification, the loss factor was also computed using the full multi-bunched beam spectrum, and it was found to agree to within <0.1 % [13].

SIMULATION PARAMETERS

At the ESRF, X-rays are delivered in many different filling patterns. The most common filling mode is the 7/8+1 (7/8 of the ring is uniformly filled with 1 single high current bunch in the middle of the gap) with 200 mA total current. However from time to time, fewer bunches with higher currents are used for the so-called timing experiments. It is in these filling patterns, high single bunch currents with multiple bunches ($N = 16$ or $N = 32$), that the power deposition is increased. The filling mode with the most significant power deposition is $N = 16$ with $I_b = 92\text{mA}/N = 5.75\text{mA}$. In this filling pattern, the bunch length has been measured to be $\sigma_z = 9.5\,\text{mm}$. For the simulations that are to follow, a symmetric bunch distribution with this σ_z is assumed, which is not completely accurate as the bunch distribution is asymmetric at these currents. However to first order this excitation pulse is sufficient.

Table 1 contains the parameters used for the simulations and following calculations for the power deposition in 16 bunch mode.

Table 1: Relevant Beam and Vacuum Chamber Parameters for the Simulations of the CPMU

Description	Value	Units
Vertical Chamber Aperture: a	6	mm
Taper Length: L	135	mm
Magnet Length: L_m	2	m
Half Gap Range: g	3-15	mm
Revolution Frequency:	350	kHz
Zero Current Bunch Length: σ_{z0}	3	mm
Current per Bunch: I_b	5.75	mA
Number of Bunches: N	16	-
Bunch Length: σ_z	9.5	mm
Resistivity of Cu. at 300 K: ρ_{300K}	1.68	x10^{-8} m
Resistivity of Cu. at 80 K: ρ_{80K}	0.28	x10^{-8} m

The CPMU magnets are blocks of Iron, coated with 50 um of Nickel and 80 µm of Copper. These complicated coating structures can be difficult to accurate simulate. As a first check, Impedance Wake 2D (IW2D) was used to compute the longitudinal impedance and therefore the loss parameter of the realistic coating structure to be compared with a pure copper block. The IW2D computations showed perfect agreement between the loss parameters of the two cases. This means that pure Copper could be used in all simulations.

The CPMU simulations can be separated into two sections: first there is the central magnet block of 2 meters. This section can be computed as a slice and simply scaled to the length of the magnet block. The second section that needs to be considered is the tapers. The chamber opening at the entrance and exit of the CPMU is 6 mm half gap in the vertical plane. This then tapers to the CPMU half gap over a length of 135 mm. A first approximation of the total power deposition in the magnets can be made by simply simulating the magnet section in IW2D and scaling with the length of the magnets, however there could be significant additional power deposition coming from the tapers, so a further simulation in CST was needed.

Power Distribution on Surface

Before computing the power deposition along the CPMU, first the power deposition perpendicular to the beam motion needs to be computed in order to determine the validity of the parallel plates model. In CST Particle Studio, two parallel plates with a width of 102 mm were simulated for the full range of gap settings. A magnetic field monitor was set to extract the field at zero frequency transversely along the plates. As the plates are flat, the projection of the field onto the surface is Gaussian, which increases with gap size. A fit of the surface Gaussian distribution is made and the results are shown in Fig. 3. For the maximum half gap of 15 mm, the sigma of the distribution on the surface is 12 mm. For the plate width of 102 mm, this means that for the most extreme case, the power distribution up to 4.25σ is included. This means that parallel plates can be modelled for the CPMU with minimal uncertainties coming from truncated tranverse magnetic field distributions.

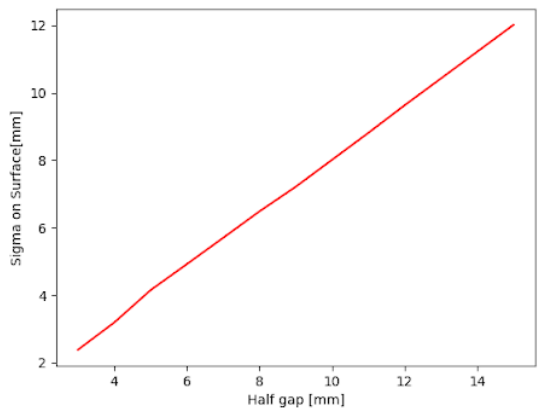

Figure 3: The sigma of the magnetic field distribution along the surface of the parallel plates perpendicular to the beam motion.

ISBN: 978-3-95450-227-1 ISSN: 2673-5490 doi:10.18429/JACoW-IPAC2022-THPOPT002

Taper Simulations

To simulate the power deposition along the CPMU, including the tapers, the 'Time Resolved Losses' feature in CST Particle Studio was used. This feature computes the power deposition as a function of time for a given lossy metal. However to make this compatible with the CPMU taper, it was necessary to slice the CPMU transversely in approximately fixed steps and assign each copper block its own material conductivity (identical for all blocks). This tedious but necessary step resulted in 76 identically defined copper blocks along the CPMU structure, with an individual result of the power deposition with time. Simply integrating this curve, multiplying by the number of bunches, dividing by f_0 and normalising to the block length was sufficient to extract the power deposition for each block. The geometry modelled in CST was a simplified model that is only representative of the perfectly constructed CPMU. This model is not accurate in the case of manufacturing or fabrication errors.

RESULTS

The results of these simulations can be found in Fig. 4. The lower plot shows a drawing of the taper geometry for the minimum gap (solid) and maximum gap (dashed) cases. The upper plot shows the power deposition as a function of the longitudinal position along the CPMU. For the central part, only 50 cm was taken (as opposed to the 2 m long magnets in reality), however as can be seen, this is enough to reach the steady state. For each of the cases shown, the power deposition was also computed in IW2D as a function of gap and the values shown were consistent with the values at the center of the geometry. As expected, the power deposition increases significantly for lower gaps and is smaller for larger gaps. It is clear that the taper angle is small enough to not create hot spots at the kinks of the taper. This allows a smooth increase of the surface temperature for small gaps.

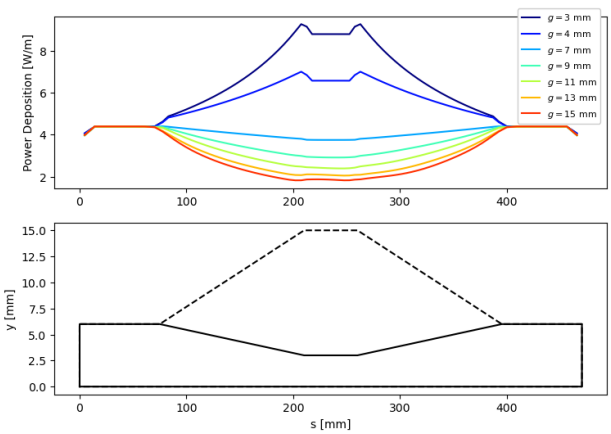

Figure 4: Power deposition as a function of the longitudinal position along the CPMU. The lower plot shows the simple geometry for minimum gap (solid) and maximum gap (dashed). The upper plot shows the power deposition for different gap settings.

From these results, the total power deposition in the CPMU can be computed. Shown in Fig. 5 is the total integral of each curve in Fig. 4 with an additional 1.95 m of the value of the central magnet added. The results were then scaled from room temperature copper to copper at 80 K.

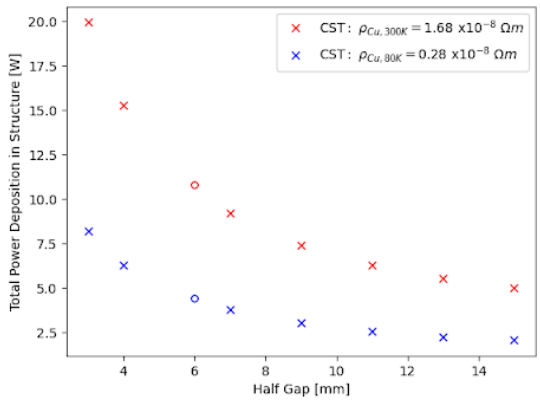

Figure 5: Total power deposited in the full CPMU structure. The original results were for copper at 300 K (red) and these were scaled to a resistivity of 80 K (blue). The circle point at a gap of 6 mm is computed from IW2D due to the fact that it is a flat parallel plate.

This peak power deposition of 20 W for a half gap of 3 mm for room temperature copper, corresponds to a temperature increase of 6 K if it was all put on the magnet blocks. However, it is only the central part of the CPMU that is at risk of demagnetisation. In this case, only the central part should be considered, therefore the temperature increase on the magnets is 5.2 K. All of these temperature increases drop quickly for a half gap of 15 mm, with temperature increases at 15 mm expected to be slightly less than 1 K. Again, this is considering perfect mechanics and therefore geometry and perfect electrical and thermal contacts between moving components. Realistic conditions could deteriorate the predicted heating.

CONCLUSIONS

The power deposition by the beam in the CPMU in 16 bunch mode was computed and a maximum power of 20 W was found. This corresponds to a temperature increase of approximately 5.2 K, significantly less than was feared. For the maximum gap setting, the temperature increase is less than 1 K.

As a result of these simulations, in the event of a failure of the cryogenic cooling, the magnets can be sent to the maximum setting and the intervention can be scheduled during shut downs, there will be no need for emergency changes to the operation schedule in order to protect the magnets.

ISBN: 978-3-95450-227-1 ISSN: 2673-5490 doi:10.18429/JACoW-IPAC2022-THPOPT002

REFERENCES

[1] "ESRF upgrade programme phase II (Orange book)", ESRF, December 2014.

[2] P. Raimondi, N. Carmignani, L. R. Carver, J. Chavanne, L. Farvacque, G. Le Bec, S. M. Liuzzo, T. Perron, S. White, "The Hybrid Multi-Bend Achromat lattice commissioning at the European Synchrotron Radiation Facility", *Phys. Rev. Accel. Beams*, to be published

[3] "Science and technology programme 2008-2017 (Purple book)", ESRF, September 2007.

[4] G. Lebec, C. Benabderrahmane, and J. Chavanne, "Simulation of NdFeB Permanent Magnets at Low Temperature", in *Proc. PAC'09*, Vancouver, Canada, May 2009, paper MO6PFP085, pp. 327–329.

[5] T. Brochard, P. M. Brumund, L. Goirand, J. Pasquaud, and S. M. White, "RF Fingers for the New ESRF-EBS Storage Ring", in *Proc. MEDSI'18*, Paris, France, Jun. 2018, pp. 11–14. doi:10.18429/JACoW-MEDSI2018-TUOPMA07

[6] C. Benabderrahmane *et al.*, "Development and Construction of Cryogenic Permanent Magnet Undulators for ESRF-EBS", presented at the IPAC'22, Bangkok, Thailand, Jun. 2022, paper THPOPT050, this conference.

[7] T. Hara *et al.*, "Cryogenic Permanent Magnet Undulators", *Phys. Rev. Spec. Top. Accelerators and Beams*, vol. 7, p. 050702, 2004. doi:10.1103/PhysRevSTAB.7.050702

[8] J. Chavanne, M. Hahn, R. Kersevan, C. A. Kitegi, C. Penel, and F. Revol, "Construction of a Cryogenic Permanent Magnet Undulator at ESRF", in *Proc. EPAC'08*, Genoa, Italy, Jun. 2008, paper WEPC105, pp. 2243–2245.

[9] CST Particle Studio, http://www.3ds.com/.

[10] N. Mounet, "The LHC Transverse Coupled Bunch Instability", EPFL, Ph.D. Thesis No. 5305, Lausanne, Switzerland, 2012.

[11] B. Zotter, S. Kheifets, *Impedances and Wakes in High Energy Accelerators*, World Scientific, 1998.

[12] A. Chao, *Physics of Collective Beam Instabilities in High Energy Accelerators*, 1st Edition, Wiley Series in Beam Physics and Accelerator Technology, 1993.

[13] G. Rumolo, "Beam Instabilities", CERN, Geneva, Switzerland, CERN Yellow Report CERN-2014-009, pp.199-220, 2014.